# A Ray-based Channel Model For MIMO Troposcatter Communications

**Ergin Dinc** **Ozgur B. Akan**
Next-generation and Wireless Communications Laboratory
Department of Electrical and Electronics Engineering
Koc University, Istanbul, 34450 Turkey.
Email: {edinc, akan}@ku.edu.tr

***Abstract*—Troposcatter communications provide a good alternative for beyond-Line-of-Sight (b-LoS) communication because it can provide reliable high data rate applications with the advancement in the modem and high power amplifiers. The employment of the high data rate applications with troposcatter communications requires the investigation of the troposcatter channels. However, available channel models for the troposcatter communications are not able to take the non-homogeneities of the air turbulence into account. Therefore, the main motivation of this paper is to develop a ray-based MIMO troposcatter channel model in which the beamwidths of the antennas are divided to small parts and, the associated delay and power of the rays are calculated in order to consider the non-homogeneities and time variations of the channel. Also, in order to show the time varying behaviour of the channel this paper provides the simulation results for the maximum data rate of the channel by using real world measurements first time in the literature.**

***Index Terms*—Troposcatter, Scattering, Channel modelling, MIMO, Maximum data rate**

## I. Introduction

Tropospheric scatter that is widely known as troposcatter, is the scattering of the propagating signals in all directions due to the irregularities in the troposphere at the particular frequency range of 1 to 20 GHz. The scattered signals are directed especially in the forward direction, but some of the signal power is directed to the receiver station. To this end, the transmitter and receiver antennas should be pointed to the radio horizon as in Figure 1. By this way, the beamdiwdts of the antennas form the troposcatter common volume where the scattered power can be received by the receiver antenna. As a result, the effects of the troposcatter can be utilized for b-LoS radio communications.

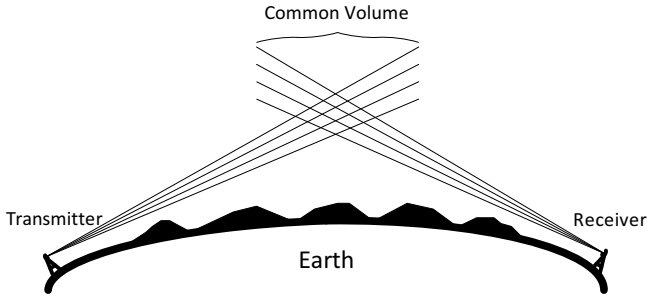


Fig. 1: Troposcatter b-LoS paths

In the past, troposcatter communication was popular for b-LoS applications because troposcatter can provide radio communication between sides having distances up to 500 km. As a result, troposcatter communication was widely used in both civilian and military applications. However, the performance of the troposcatter links degrades due to high path loss resulting from the high path length and more importantly scattering. Therefore, the b-LoS troposcatter applications were replaced by Satellite Communications (SATCOM).

Since SATCOM has capacity problems in regions having low satellite coverage and introduces excessive transmision delays, especially military applications require an alternative technique for b-LoS communications. As a result, the troposcatter communication regains its popularity because it can provide reliable and high data rate b-LoS links with the advancement in the troposcatter equipments and communication techniques. The state-of-the-art troposcatter modems that can provide up to 22 Mbps, and solid-state amplifiers which can reach up to 2 kW transmit powers are available [1]. Also, the evolution of the packet based networking techniques can provide reliable communication with variable-capacity in troposcatter systems [1]. In addition, MIMO communication techniques can be utilized in order to further increase the performance of the troposcatter systems.

In order to use the troposcatter communication efficiently for high data rate applications, the investigation of the channel characteristics is required. However, the available troposcatter channel models do not provide effective modelling of the time varying behaviour of the complex air turbulence. Therefore, the main purpose of this work is to develop a detailed MIMO channel model for troposcatter communication. To this end, a ray-based technique is proposed in order to model the time variations and non-homogeneities of the channel. In addition, the simulation results for the maximum data rate of the troposcatter channel are presented in order to show the time varying behaviour of the channel.

The remaining of the paper is organized as follows. Section II provides the summary of available troposcatter models and the contributions of this work. Troposcatter geometry and path length calculations are introduced in Section III. Section IV covers the path loss calculations for troposcatter communications. In Section V, the maximum data rate equations for MIMO troposcatter channel are presented, and lastly Section

VI includes the simulation results for the maximum data rate distribution of the channel.

## II. Related Work and Contributions

Since troposcatter channel can provide a single-hop long distance communication with high reliability and confidentiality, it can be utilized especially for military applications in order to provide high capacity. As a result, the investigation of the channel properties of the troposcatter communications is required. To this end, there are some channel models for troposcatter. Firstly, the statistical methods are used to predict the annual and worst month transmission losses of the troposcatter links by utilizing empirical statistical averages [2], [3]. However, these statistical methods are inadequate to model the fast variations in the channel.

In addition to the statistical models, the analytical expressions for the delay power spectrum of the troposcatter links are provided in [4]. This technique indicates that the envelope of the delay power spectrum obeys the Rayleigh distribution. Based on this result, Rayleigh distributed delay tapped troposcatter channel models are developed in order to investigate the bit error rate of the troposcatter links [5], [6]. However, these models are inadequate to model the complex nature of the air turbulence because the scattering cross section in these models depends only on the scattering angle.

To this end, the main motivation of this work is to develop MIMO troposcatter channel model in order to consider the effect of the fluctuations and non-homogeneities in the air turbulence because available troposcatter channel models are inefficient to model the air turbulence. Therefore, we use a ray-based technique to predict the received signal power and the variations of the air turbulence is modelled with Kolmogorov spectrum technique using the Rayleigh scattering approximation [7], [8]. The variations in the troposcatter common volume are taken into account by using the changes in the refractive index of the air that is derived from real world water vapour mixing ratio measurements [9].

In addition to the variations in air turbulence, our method also considers the effects of the polarization by using Stoke's matrix [8]. As a result, this work provides a comprehensive theoretical model for MIMO troposcatter communication that considers the variations in the layer and the polarization of the scattered signals. Also more importantly in order to show the variations in the channel, the results for maximum data rate simulations by using real world measurements are presented first time in the literature for MIMO troposcatter communication.

## III. Troposcatter Geometry

The path loss calculations require the investigation of the channel geometry because they depend on the path lengths and delay spreads. To this end, the geometry of the troposcatter channel can be seen from Figure 2 and the parameters used in Figure 2 are listed and described in Table I.

Troposcatter wave propagation suffers from high path loss due to the long path lengths. Therefore, low elevation angles

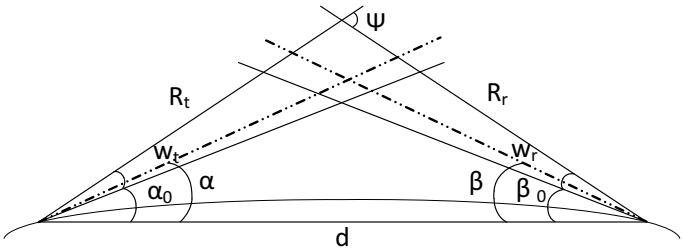


Fig. 2: The geometry of the troposcatter link

| | |
|---|---|
| d | Horizontal distance between transmitter and receiver |
| R | Distance between transmitter and scatter point |
| S | Distance between receiver and scatter point |
| $\alpha_0$ | Elevation angle of the antenna at the transmitter |
| $\beta_0$ | Elevation angle of the antenna at the receiver |
| $\alpha$ | Elevation angle of the instantaneous ray at the transmitter |
| $\beta$ | Elevation angle of the instantaneous ray at the receiver |
| $\Psi$ | Scatter angle |
| $w_t$ | Beamwidth of the transmitter |
| $w_r$ | Beamwidth of the receiver |

TABLE I: The parameters in troposcatter geometry

are used in the troposcatter links in order to keep the path length as low as possible because $1^\circ$ increase in the elevation angle can result in 9 dB decrease in the transmitted power. In addition, even very low increase in the elevation angle can cause 1 km difference in the height of the troposcatter common volume and ascending height of the troposcatter common volume can increase the path loss due to low density of scatterers at higher heights. As a result, the antennas should be pointed to the radio horizon in order to decrease the path loss. To this end, the appropriate values for the elevation angles can be given as [2]

$$\alpha_0 = \beta_0 = \frac{d}{2R_0} \text{ rad}, \tag{1}$$

where $R_0$ represents the effective radius of the earth. Since troposcatter antennas use very low elevation angles, the curvature of the earth becomes important in the path length calculations. To this end, the effective radius of the earth can be given as

$$R_0 = kR \text{ km}, \tag{2}$$

where $R$ is the radius of the earth ($\approx 6370$ km) and $k$ represents the effective earth radius factor for median refractivity conditions that can be taken as $4/3$ [3].

The total path length in the troposcatter link is equal to the summation of the distance between the scattering point and transmitter ($R$), and the distance between the scattering point and receiver ($S$). The relationship between these distances and horizontal distance can be given as:

$$\frac{d}{\sin(\Psi)} = \frac{R}{\sin(\beta)} = \frac{S}{\sin(\alpha)}, \tag{3}$$

where scattering angle is given by $\Psi = \alpha + \beta$.

In order to find the delay spread of the signals, it is required to find the difference between the signal path and the reference

path. To this end, the shortest path is assumed as the reference path in the troposcatter links because the troposcatter link has no line-of-sight (LOS) component at high distances.

The path length difference between the reference and any path is utilized to calculate the delay spread. To this end, the path length difference between an instantaneous ray and the horizontal path is given by [2]

$$\Delta d = R + S - d = \frac{1}{2}\alpha\beta d \text{ km}, \tag{4}$$

and (4) can be modified to determine the path length difference between any two paths as [2]

$$\Delta d_{12} = \frac{d}{2}(\alpha_1\beta_1 - \alpha_2\beta_2) \text{ km}. \tag{5}$$

Since the reference path in troposcatter links is the shortest one, the second path in (5) is associated with the elevation angles of $\alpha_0$ and $\beta_0$ given by (1). Therefore, this path is assumed to have zero delay and the relative delay spreads of the other rays are calculated with respect to the reference. The path length and delay calculations will be used in Section V in order to predict the power of the received signal.

## IV. Troposcatter Path Loss

Troposcatter makes the most of scattered signal energy directed in the forward direction. However, some portion of the signal energy is scattered towards to the receiving station. Since the scattering of the propagating signals strongly depends on the distribution and size of the scattering particles, the variations of the air turbulence play an important role in the wave propagation. To this end, scattering by air turbulence is modelled and expressions for the power of the scattered signals is presented in this section. At the end, the results of the power calculations are used to predict the received power at the receiver in order to determine the maximum data rate of the channel as will be discussed in Section V.

Since the main motivation of this work is to provide a channel model which considers the non-homogeneities and variations in the air turbulence, we use a ray-based technique that divides the beamwidths of the antennas to small parts and calculate corresponding delay and power of the rays. By this way, the rays corresponding to different regions in the troposcatter common volume are subjected to different power attenuations. Therefore, the ray-based model takes into account the non-homogeneities of the channel. In addition, since the distribution of the scatterers is modelled with the water vapour mixing ratio measurements, the ray-based model is able to take the variations in the channel into consideration.

The ray-based technique requires differential power calculations and better model for the scattering cross section. To this end, the power calculations can be done by starting with the bistatic radar range equation

$$P_r = \frac{P_t G_t G_r \sigma_V \lambda^2 \rho}{(4\pi)^3 R^2 S^2} \text{ W}, \tag{6}$$

where $\lambda$ is the wavelength and $P_{r,t}$ represent the received and transmit power, respectively. In addition, $\sigma_V$ is the scattering cross section. $G_t$ and $G_r$ are the antenna gains for transmitter and receiver, respectively. $\rho$ represents the polarization mismatch factor and the details of these parameters are given in the following subsections.

### A. Scattering Cross Section

The troposcatter common volume contains scattering particles with different sizes and shapes, and the sizes of the scatterers are generally in the order of 1-10 $\mu$m. As a result, the wavelengths of the signals having frequencies 1 to 20 GHz in which the effect of the troposcatter is considerable, are much larger in size compared to the scattering particles. Therefore, Rayleigh scattering approximation, which is valid when the sizes of the scatterers are much smaller than the wavelength, can be used to model the scattering event [7].

Kolmogorov spectrum technique, which depends on the variation of the index of refraction, can be used to model non-homogeneities and variations of the air turbulence. Therefore by using Rayleigh scattering approximation and Kolmogorov spectrum technique, the differential scattering cross section can be represented as [7]

$$\sigma_V = 2\pi k^4 \cos(\Psi)^2 dV_c \Phi(k_s) \text{ m}^2, \tag{7}$$

where $dV_c$ is the differential scattering volume. $k$ is the wave number given by $2\pi/\lambda$ and fourth power dependence of the wavelength comes from Rayleigh scattering approximation. $cos^2(\Psi)$ represents the effect of the scatter angle on the signal power. In addition, $\Phi(k_s)$ represents the Kolmogorov spectrum that can be given as [7]

$$\Phi(k_s) = 0.33\pi^3 C_n^2 (2k\sin(\Psi/2))^{-11/3} \text{ m}^3, \tag{8}$$

where $C_n$ represents the fluctuations in the index of refraction and $k_s = 2k\sin(\Psi/2)$.

The fluctuations of the index of refraction ($C_n$) is derived from the water vapour mixing ratio measurements provided by NASA Langley Research Center in order to observe the time variations in the channel [9]. To this end, refractivity of the air is derived by using water vapour mixing ratio and then the fluctuations of the index of refraction will be calculated directly using the refractivity of the air that is given by [10]

$$N = \frac{77.6}{T}(P + 4810 \times e/T) \text{ N-units}, \tag{9}$$

where $T$ represents the temperature of the air in Kelvin and $P$ represents total atmospheric pressure in mb and, $e$ represents vapour pressure that can be derived by

$$e = \frac{P}{\varepsilon}\omega \text{ mb}, \tag{10}$$

where $\omega$ represents the water vapour mixing ratio of the air that means the amount of water in air in g/kg and the molecular mass ratio of water vapor to air ($\varepsilon$) can be taken as $0.622$ [11].

The relationship between the refractive index and refractivity can be determined with the following equations [10]:

$$N = (n-1) \times 10^6 \text{ N-units},$$
$$\frac{\partial N}{\partial z} = \frac{\partial n}{\partial z} \times 10^6 \text{ N-units/m}. \tag{11}$$

Lastly, differential scattering volume can be given as [8]

$$dV_c = \frac{R^2 S^2 (dw)^2}{\sqrt{R^2 + S^2}\sin(\Psi)} \text{ m}^3, \tag{12}$$

where $dw$ is the differential beamwidth of the rays.

### B. Troposcatter Antennas

Since troposcatter channel suffers from high path loss due to the long path lengths and scattering, low beamwidth reflector antennas having $2.4$ to $3$ m diameters are used in troposcatter communication. As a result, the antennas can provide high antenna gains thanks to high apparatus areas. In addition, low beamwidths provide signals to spread less, so that the resulting delay spread and path loss are lower.

Since troposcatter antennas use low beamwidths around $3$ to $10$ mrad according to the path and atmospheric conditions, the type of the antenna has low effect in the simulations [3]. Therefore, the troposcatter antennas are modelled as isotropic antennas and the antenna gains can be found by [1]

$$G_{t,r} = 10\log\left[\eta_{ant}\left(\frac{\pi D_{ant}}{\lambda}^2\right)\right] \text{dBi}, \tag{13}$$

where $\eta_{ant}$ is antenna efficiency, $D_{ant}$ is antenna reflector diameter. (13) yields antenna gain of $41.5141$ dBi for the carrier frequency of $4.7$ GHz, antenna efficiency of $0.65$ and antenna diameter of $3$ m that are used in this work.

### C. Polarization of The Scattered Waves

Polarization has substantial influence in the scattering process because randomness of the troposcatter common volume generally makes the scattered signal to have elliptically polarized notwithstanding its previous polarization [7]. Therefore, the polarization of the scattered rays is nearly random due to the randomness of the air turbulence.

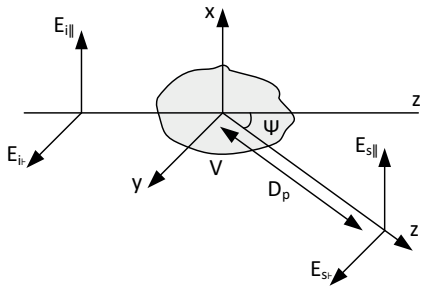


Fig. 3: Geometry of the scattering

Since the scattering particles are much smaller in size with respect to the wavelength, the shape of the scattering particles are assumed to have spherical shapes. Therefore by using Rayleigh scattering approximation for 2D troposcatter links, the polarization of scattered waves at some distance from the scattering point can be determined by Stoke's matrix that can be represented as [7]

$$\begin{pmatrix} E_{s\perp} \\ E_{s\parallel} \end{pmatrix} = \begin{pmatrix} e^{ikr} \\ R \end{pmatrix} \begin{pmatrix} \cos(\Psi) & 0 \\ 0 & 1 \end{pmatrix} \begin{pmatrix} E_{i\perp} \\ E_{i\parallel} \end{pmatrix} \tag{14}$$

where $E_s$ represents the polarization of the signal at a distance $R$ from the scattering point and $E_i$ represents the polarization of the wave at the scattering point as shown in Figure 3.

The polarization mismatch factor between the receiver antenna and the received ray can be determined by

$$\rho = |\hat{e}_s \hat{e}_r|^2, \tag{15}$$

where $\hat{e}_r$ is the polarization vector of the receiver antenna and $\hat{e}_s$ is the polarization vector of the scattered wave that can be determined by (14).

## V. Maximum Data Rate

Since troposcatter communication introduces high path loss and fast fading due to the fluctuations in the air turbulence, diversity techniques should be employed in order to increase the performance of the system. To this end, we use 2x2 space-frequency diversity in the troposcatter communication. As a result, horizontally spaced antennas provide increase in the received power and frequency separation keeps the interference between the cross antennas low. The appropriate horizontal and frequency separation between the antennas are utilized in order to provide different antenna pairs to have low correlation as suggested by [3]. Therefore, the maximum data rate of the system in troposcatter links utilizes MIMO capacity calculations provided by [12] and the channel gain matrix is formed by the proposed ray-based technique by implementing the method for the each antenna pair.

For the maximum data rate or capacity calculations, the channel capacity of the troposcatter communication can be given as [12]

$$C = \sum_{i=1}^{R_H} B\log_2\left(1 + \frac{\gamma_i}{M_t})\right) \text{ bps}, \tag{16}$$

where $\gamma_i = \sigma_i^2 P_t/N$ and $\sigma_i$'s are the nonzero eigenvalues derived from singular value decomposition of channel gain matrix $(H)$ and $N$ represents the noise power. In addition, $R_H$ represents the number of nonzero singular values of $H$ and $M_t$ is the number of transmitter antennas.

In order to form the channel gain matrix, the received power of the antennas will be used. To this end, the rays having the same delay component are added to each other and the delay power spectrum of the troposcatter channel is formed by using the the delay spread and differential power calculations as discussed in Section III and IV.

In order to calculate the capacity of the troposcatter communication, the noise can be modelled as thermal noise due to high operating frequencies of the modern troposcatter systems. To this end, the noise power is given by

$$N_0 = kBT \text{ W}, \tag{17}$$

where $T$ is temperature in K, $B$ is the bandwidth of the signal and $k$ is the Boltzmann constant. Since we are using high gain antennas the effective noise in the system will be the thermal noise times the antenna gain of the receiver. Therefore, the noise power $(N)$ becomes $N = N_0 G_R$.

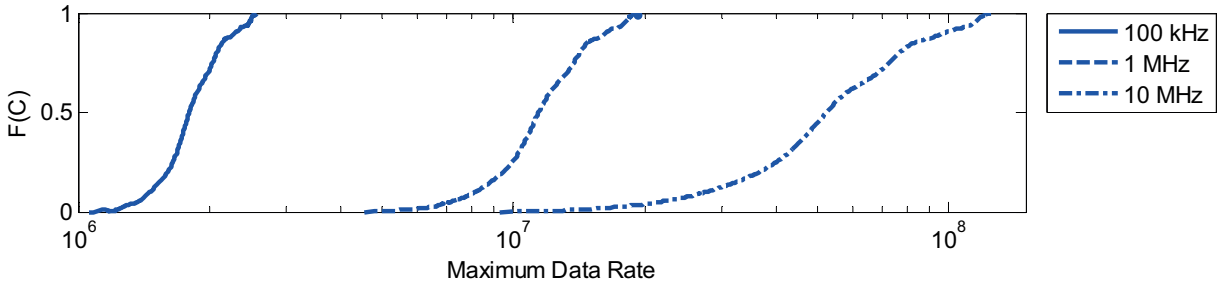


Fig. 4: The cumulative distribution function of maximum data rate for different bandwidths in 2x2 MIMO troposcatter channel

## VI. Simulation Results For Maximum Data Rate

Up to now, the ray-based channel model for MIMO troposcatter communication has been formed and now, the simulation results for the maximum data rate of the channel is presented by implementing the proposed method in MATLAB.

The troposcatter channel parameters that were used in the simulations can be found in Table II. In addition to the channel parameters, the troposcatter antennas are modelled with linear horizontal polarization. Also, the maximum data rate calculations are performed with real world data by using the the received power of the antennas coming from the proposed ray-based technique.

| **Parameter** | **Value** | **Unit** |
|---|---|---|
| Frequency ($f$) | 4.7 | GHz |
| Horizontal distance ($d$) | 170 | km |
| Transmit power ($P_t$) | 1 | kW |
| Antenna gains ($G_{t,r}$) | 41 | dBi |
| Elevation angles ($alpha_0$,$beta_0$) | 10 | mrad |
| Antenna beamwidths ($w_{1,2}$) | 10.5 | mrad |
| Frequency separation ($\Delta f$) [3] | 30 | MHz |
| Horizontal spacing ($\Delta h$) [3] | 10 | m |

TABLE II: Troposcatter communication parameters

Figure 4 shows the cumulative distribution function of maximum data rate of the 2x2 MIMO troposcatter links. As noticed from Figure 4, the distribution of the maximum date rate for 100 kHz is almost Gaussian. However, as the bandwidth of the troposcatter link increases, the distribution of the maximum data rate changes. At high bandwidths, the distribution of the maximum data rate is close the Rayleigh distribution due to the suppressing effect of the noise power because the noise power depends directly on the bandwidth as in (17). Furthermore, the span of the achievable data rates increase with the bandwidth. Therefore, increasing bandwidth makes the troposcatter channel less stable.

In addition, the increase in the maximum data rate becomes less at higher bandwidths as noticed from Figure 4 because the effect of the noise become more dominant. Therefore, we can conclude that the suppressing effect of the noise introduces an important boundary for the bandwidth of troposcatter systems. However, MIMO troposcatter communication is still able to provide high data rates more than 10 Mbps at 70% of the time for 1 MHz bandwidth and more than 22 Mbps at 90% of the time for 10 MHz bandwidth as also stated in [1] as noticed in Figure 4. Therefore, high data rate b-LoS applications can utilize troposcatter communication.

## VII. Conclusion And Future Work

In this paper, we proposed a ray-based MIMO troposcatter channel model in order to model the fluctuations and non-homogeneities of the air turbulence. In addition, the simulation results for the maximum data rate of the 2x2 MIMO troposcatter channel by using real world water vapour mixing ratio measurement are presented. The results of this paper can be used as design guidelines for MIMO troposcatter systems and the proposed technique can be used to further investigate the properties of the troposcatter channel. To this end, the proposed ray-based model can be extended to model the effects of the rain and cloud attenuation and also, the receiver can be optimized to decrease the received power loss due to the polarization mismatch.

## References

[1] L. Bastos, H. Wietgrefe, "Tactical troposcatter applications in challenging climate zones," *MILCOM 2012*, pp. 1-6, 2012.
[2] G. Roda, Troposcatter Radio Links. Artech House Publishers, 1988.
[3] "Propagation prediction techniques and data required for the design of trans-horizon radio-relay systems", *ITU-R Recommendations P.617-2*.
[4] P. Bello, "A Troposcatter Channel Model," *IEEE Transactions on Communication Technology*, vol. 17, no. 2, pp. 130-137, April 1969.
[5] Zhao Yu, Chen Xi-hong, "Research on MRC based on Rake receiver in troposcatter communication," *Consumer Electronics, Communications and Networks*, pp. 4342-4345, 2011.
[6] Yi Wang, Yingwu Fang, Xinyu Da, Wei Jin, "Study on Modeling of Troposcatter Communication and MRC in Correlated Channel by Matlab," *WiCOM*, 2008.
[7] A. Ishimaru, Wave Propagation and Scattering in Random Media. IEEE Press Series on Electromagnetic Wave Theory, Wiley, 1999.
[8] L. Tsang, J. A. Kong, K. Ding, Scattering of Electromagnetic Waves: Theories and Applications, John Wiley & Sons, 2000.
[9] NAMMA LASE, NASA EOSDIS GHRC DAAC, http://ghrc.msfc.nasa.gov/index.html. Accessed on Jan 30, 2013.
[10] R. A. Paulus, "Evaporation duct effects on sea clutter," *IEEE Trans. Antennas Propag.*, vol. 38, no. 11, pp. 1765-1771, Nov 1990.
[11] G. Ehret, C. Kiemle, W. Renger, and G. Simmet, "Airborne remote sensing of tropospheric water vapor with a near-infrared differential absorption lidar system," *Applied Optics*, vol. 32, pp. 4534-4551, 1993.
[12] A. Goldsmith, Wireless Communications, Cambridge University Press, 2005.